

CLOSED SURFACE RECONSTRUCTION IN X-RAY TOMOGRAPHY

Charles Soussen, Ali Mohammad-Djafari

Laboratoire des Signaux et Systèmes (CNRS – SUPÉLEC – UPS)
Supélec, Plateau de Moulon, 91192 Gif-sur-Yvette Cedex, France

ABSTRACT

We study the 3D reconstruction of a binary scene from X-ray tomographic data. In the special case of a compact and uniform object lying in a uniform background, the scene is entirely defined by the object surface. Then, we select parametric surface models, and we directly estimate their parameters from the data. After showing the ability of spherical harmonics and first order splines (polyhedra) to recover complex shapes, we develop an original method to estimate their parameters without using a voxel representation of the scene (object and background). Reconstructions are based on the optimization of regularized criteria, which account for the surfaces local smoothness. We use local optimization schemes, and we put the stress on their algorithmic aspects. We finally show the performance of the method on a set of incomplete synthetic data.

1. INTRODUCTION

The present work is about 3D shape reconstruction from X-ray tomographic data. We consider a scene composed of a compact and uniform object lying in a uniform background. Under those assumptions, we model the object by its closed surface \mathcal{C}^* , which is entirely included in the zone of interest. Such situations are encountered in nondestructive testing (NDT) applications, in which \mathcal{C}^* represents an air fault included in a metal area [1]. In those applications, the absorption coefficients and the density values of the materials are generally known. Without loss of generality, we can then assign the values 1 and 0 to those regions. And the density function of the scene writes:

$$f(x, y, z) = \begin{cases} 1 & \text{if } (x, y, z) \text{ lays inside } \mathcal{C}^*, \\ 0 & \text{otherwise.} \end{cases} \quad (1)$$

Voxel based approaches, which discretize the scene by a set of binary cubic elements, and then estimate their values, have been extensively used in tomographic image reconstruction [1]. However, a surface based approach appears more appropriate in our context, since it naturally takes advantage of the object compactness assumption [2, 3, 4]. More precisely, the aim of this approach is to directly reconstruct \mathcal{C}^* by means of a deformable closed surface. In the following, we consider a parametric model $\mathcal{C}_{\mathbf{x}}$, where \mathbf{x} belongs to a subset of \mathbb{R}^k . Reconstruction of \mathcal{C}^* reduces to the estimation of \mathbf{x} from the data: the reconstructed surface is then $\hat{\mathcal{C}} = \mathcal{C}_{\hat{\mathbf{x}}}$, where $\hat{\mathbf{x}}$ stands for the parameter estimate. This approach appears especially adequate when the number of data is limited, since it affords a drastic reduction of the scene parameterization. Such situations often arise in NDT applications, in which both number and angles of projections are limited due to physical acquisition constraints.

The paper is organized as follows. Section 2 states the data modeling and specifies the surface reconstruction framework. We

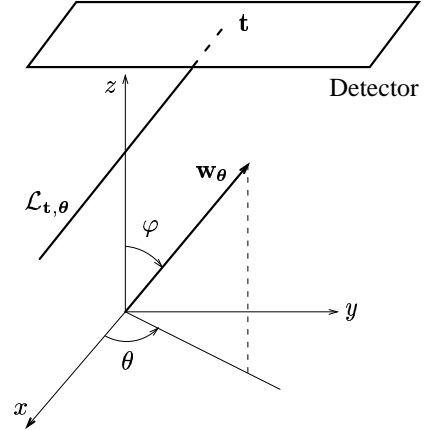


Fig. 1. Line projection parameters; $\theta = (\theta, \varphi) \in [0, 2\pi] \times [0, \pi]$.

use the regularization theory, and we define the maximum *a posteriori* (MAP) estimator of parameters \mathbf{x} by accounting for prior information on the local smoothness of $\mathcal{C}_{\mathbf{x}}$. In Section 3, we discuss the choice of the parametric model, and we study the specific case of global harmonics and local splines. Section 4 investigates the reconstruction of first order splines, *i.e.*, polyhedra, by estimation of their vertices coordinates. Optimization of the posterior energy is done by accurate local schemes, based on the exact calculation of the surface projection and its derivatives with respect to (w.r.t.) the parameters. We finally illustrate the polyhedral method performance on a set of synthetic data in Section 5.

2. PROBLEM STATEMENT

2.1. Measurement modeling

The X-ray transform of function $f(x, y, z)$ is defined by its line integrals. Using equation (1), a projection of the scene writes:

$$p_{\theta}(\mathbf{t}) = \int_{\mathcal{L}_{\mathbf{t}, \theta} \cap \mathcal{C}^*} dl, \quad (2)$$

where $\mathcal{L}_{\mathbf{t}, \theta}$ stands for the projection ray. It depends on the spherical angles $\theta = (\theta, \varphi)$ and the detector position \mathbf{t} , illustrated on Figure 1. To summarize the projection modeling, we append all scalar projection data in a vector \mathbf{d} . Then, we model the direct problem by use of the projection operator \mathcal{A} :

$$\mathbf{d} = \mathcal{A}(\mathcal{C}^*) + \mathbf{n}, \quad (3)$$

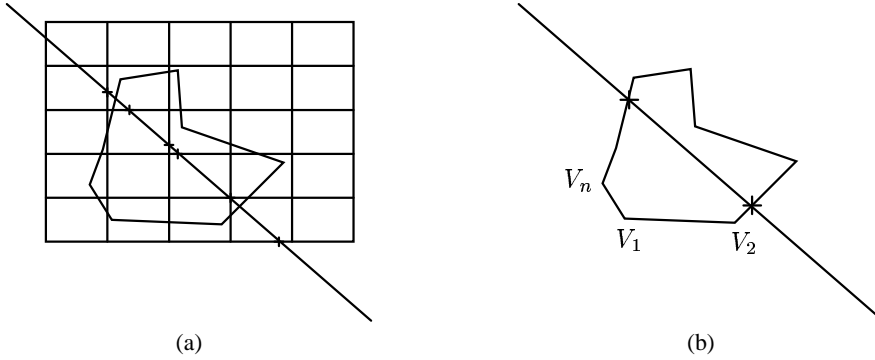


Fig. 2. 2D case: evaluation of a closed polygon projection. (a) Approximate numerical calculation by discretization of the scene into pixels. (b) Exact *analytic* calculation, based on intersections between the projection ray and the polygon edges.

where the noise \mathbf{n} accounts for the uncertainty of the scene modeling and the data acquisition errors. In particular, a more realistic model would involve band projections instead of line projections [4]. For the sake of simplicity, \mathbf{n} is assumed identically independently distributed, white and Gaussian.

2.2. Surface reconstruction scheme

Given a surface parameterization $\mathcal{C}_{\mathbf{x}}(\mathbf{x} \in \mathbb{R}^k)$, the reconstruction problem requires the estimation of $\hat{\mathbf{x}}$ from the data. In NDT applications, this problem is ill-posed because of the scarcity of the data. Indeed, both number and angles of projections are limited. We then use the regularization theory and the Bayesian inference framework. The MAP estimate, denoted by $\hat{\mathbf{x}}$, is obtained by minimization of the compound energy:

$$\hat{\mathbf{x}} = \arg \min \{ \mathcal{J}(\mathbf{x}) = \|\mathbf{d} - \mathcal{A}(\mathcal{C}_{\mathbf{x}})\|^2 + \lambda \mathcal{R}(\mathbf{x}) \}. \quad (4)$$

Criterion \mathcal{J} is the sum of a fidelity to data term and a regularization term that enforces the local smoothness of $\mathcal{C}_{\mathbf{x}}$. The specification of functional \mathcal{R} clearly depends on the parameterization $\mathcal{C}_{\mathbf{x}}$, but it is generally related to its local curvature [4].

3. CLOSED SURFACE PARAMETRIC MODELING

Closed surface models have been extensively used in image segmentation and computer vision applications, with the development of active surfaces, but more rarely in image reconstruction. In this field, the pioneering works involve very simple parametric shapes depending on a few number of parameters [2, 3]. Examples of such coarse models for a closed surface are ellipsoids and super ellipsoids, specified by less than 10 parameters. Although such general models retrieve the global spatial frequencies of a surface, the variety of generated shapes is limited. One then needs to define more complex models to reconstruct highly nonconvex surfaces. Among them, we distinguish local and global ones, in the sense that each parameter does or does not only control a local portion of the contour. Classical examples of local shapes are Bezier and spline surfaces. Such parameterizations generate efficiently smooth surfaces with local high frequency features. In the following, we start by a description of global harmonic surfaces, which yield a simple procedure to reconstruct coarse surfaces.

3.1. Harmonic surfaces

Among global surfaces, we select spherical harmonic developments (see [5] for their use in image segmentation), since they yield non intersected surfaces under specific assumptions. Using spherical angles associated to a fixed coordinate system (see Figure 1 for definition of spherical angles), we define surface $\mathcal{C}_{\mathbf{x}}$ by

$$\mathbf{M}(\boldsymbol{\theta}) = \mathbf{O} + \rho(\boldsymbol{\theta}) \mathbf{w}_{\boldsymbol{\theta}}, \quad \boldsymbol{\theta} \in [0, 2\pi] \times [0, \pi], \quad (5)$$

where \mathbf{O} stands for the surface center. Then, we consider the harmonic development of function $\rho(\boldsymbol{\theta})$, truncated at the L -th order:

$$\rho(\boldsymbol{\theta}) = \sum_{l=0}^L \sum_{|k| \leq l} x_l^k \rho_l^k(\boldsymbol{\theta}), \quad (6)$$

where ρ_l^k are the spherical harmonic functions, linked to Legendre polynomials. We practically select a low order L , and we simply estimate $\mathbf{x} = \{x_l^k, |k| \leq l \leq L\}$ in the least square sense. Including the linear constraint " $\forall \boldsymbol{\theta}, \rho(\boldsymbol{\theta}) \geq 0$ " is of interest, since it leads to star-shaped, thus unintersected surfaces. The practical difficulty relies on the projection calculation, which is approximate. Such approximation can be done either by computing the exact projections of a spline approximation of the surface, or by a discretization of the scene volume into binary voxels [6] (see Figure 2). We favor the first one, which is simple and offers a limited parameterization of the approximated scene.

In practice, spherical harmonics are modeled w.r.t. a system of inertia axes estimated from the data, prior to the surface reconstruction stage. Such estimation is done by a moment based method [7].

3.2. Local surfaces

Local parametric surfaces can efficiently model inhomogeneous closed shapes. Among them, we favor splines and we estimate the position of their control points $\mathbf{x} = \{V_1, \dots, V_n\}$ [4]. The interest of this model rests on the *exact* computation of its projections $\mathcal{A}(\mathcal{C}_{\mathbf{x}})$. The spline order is linked to the degree of locality of the control points, and then to the order of derivability of the surface w.r.t. its arc lengths. For example, a first order spline, *i.e.*, a polyhedron is piecewise affine. Points V_j are identical to the polyhedron vertices, and they only control their connected faces. In the following, we choose first order splines because both calculations

of their projections $\mathcal{A}(\mathcal{C}_{\mathbf{x}})$ and their derivatives $\nabla \mathcal{A}(\mathcal{C}_{\mathbf{x}})$ are very straightforward. Indeed, those operations are based on the evaluation and the derivation of the intersection between a projection ray and a face of the polyhedron, as pointed out on Figure 2 (b).

4. FIRST ORDER SPLINES RECONSTRUCTION

Polygons and polyhedra have been used in several ways for reconstruction purposes. First, Milanfar *et al.* studied the reconstruction of a polygon by a moment based approach [7]. Although it affords an exact reconstruction when enough projections are available, this approach is not suited to the case of noisy and limited data, and it can only reconstruct polygons with very few vertices ($n \leq 5$). Later, researchers have proposed a regularized approach to reconstruct polygons with a great number of vertices [4, 8]. 3D extensions have been developed in several manners [6, 9, 10]. In [6], the authors use an approximate calculation of the model projections based on a voxel representation of the scene (see Figure 2 (a)), whereas in [9, 10], we have favored direct computation of projections, in order to limit the scene parameterization.

4.1. Polyhedron modeling

Manipulation of polyhedra is complex since a polyhedron not only depends on its vertices V_1, \dots, V_n , but also on the composition of its faces. With fixed triangular faces, the shape is controlled by $\mathbf{x} \equiv \{V_1, \dots, V_n\} \in \mathbb{R}^{3n}$. Bayesian estimation is done in the MAP sense by minimization of criterion

$$\mathcal{J}(\mathbf{x}) = \|\mathbf{d} - \mathcal{A}(\mathbf{x})\|^2 + \lambda \sum_{j=1}^n \kappa_j(\mathbf{x}), \quad (7)$$

where the regularization term penalizes high values of the local curvatures $\kappa_j(\mathbf{x})$ of $\mathcal{C}_{\mathbf{x}}$ at its vertices V_j . In practice, the choice of λ is empirical: low values tend to yield self intersected shapes, whereas high values preserve local regularity. Exact local curvatures of polyhedra are actually undefined since the surface is not twice differentiable w.r.t. its arc lengths. However, we can define approximate curvatures. Possible bases to this definition are the distance from V_j to the center of gravity of its neighbors, the solid angle at V_j , or a combination of both. For sake of simplicity, we choose the solid angle $A_j(\mathbf{x})$ and we define $\kappa_j(\mathbf{x}) = 1 + \cos(A_j(\mathbf{x})/2)$.

4.2. Optimization schemes

Whatever the definition of curvatures, criterion \mathcal{J} is usually non-convex and multimodal since the projection operator is nonlinear (it may also be non differentiable) and the fidelity to data term $\|\mathbf{d} - \mathcal{A}(\mathbf{x})\|^2$ is itself generally nonconvex. To obtain accurate results in a reasonable computational time, we select local deterministic algorithms with high quality initializations. We practically use a prior harmonic reconstruction to yield the initial solution.

Simple local algorithms are gradient descent techniques on \mathbf{x} , and block coordinate descent techniques, which iteratively estimate the vertices V_j while the position of all other vertices remain fixed (Gauss-Seidel based approaches). The second are of interest, since they afford a test of self intersection of the polyhedron by updating its projections [10]. However, their numerical burden turn out to be important, and we favor gradient techniques on \mathbf{x} contrary to the 2D case. All local algorithms need the calculation of

Evaluate $\varepsilon_j, \varepsilon'_j$, the exterior properties of V_j, V'_j .
 Extract local polyhedra $\mathcal{C}_{\partial j}$ and $\mathcal{C}'_{\partial j}$.
 Decompose $\mathcal{C}_{\partial j}$ as the union of tetrahedra $\mathcal{U}\mathcal{T}_\tau$.
 Compute exact projections $\mathcal{A}(\mathcal{C}_{\partial j}) = \sum \mathcal{A}(\mathcal{T}_\tau)$.
 Decompose $\mathcal{C}'_{\partial j}$ and compute $\mathcal{A}(\mathcal{C}'_{\partial j})$.
 Do $\mathbf{p} = \mathbf{p} + \varepsilon'_j \mathcal{A}(\mathcal{C}'_{\partial j}) - \varepsilon_j \mathcal{A}(\mathcal{C}_{\partial j})$.

Table 1. Update of the polyhedral projections \mathbf{p} when a single vertex V_j is moved from positions V_j to V'_j .

$\nabla \mathcal{J}$, and then $\nabla \mathcal{A}$, which is related to the projection update procedure (see Table 1). When a single vertex (say V_j) is moved to a new position $V'_j = V_j + \delta V_j$, we simply extract two local polyhedra $\mathcal{C}_{\partial j}$ and $\mathcal{C}'_{\partial j}$ formed by V_j (respectively V'_j) and its neighbors, and then compute their exact projections. Such extraction is the basic idea of updating the polyhedron projections. The update algorithm depends on the exterior properties of V_j and V'_j , described by parameters ε_j and $\varepsilon'_j = \pm 1$. Namely, ε_j is set to 1 if and only if $\langle V_j G_j, \mathbf{N}_j \rangle \leq 0$, where G_j is the center of gravity of the neighbors of V_j and \mathbf{N}_j is the approximate exterior normal vector to $\mathcal{C}_{\mathbf{x}}$ at V_j . Projections of local polyhedra are evaluated analytically by their decomposition into a set of tetrahedra, whose projections have a direct analytic expression.

5. SIMULATION RESULTS

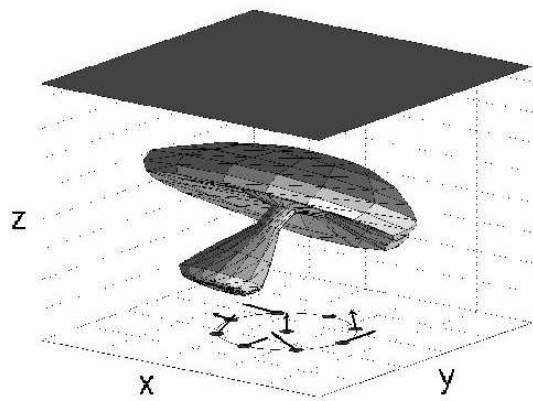
Simulations are done on a set of synthetic data, composed of 9 limited angled projections of a complex surface \mathcal{C}^* , whose signal to noise ratio is equal to 20 dB (see Figure 3). The difficulty lays in the non convexity of \mathcal{C}^* and the large variety of its curvatures. Convex initializations do not lead to accurate results since they only retrieve the low frequency characteristics of \mathcal{C}^* . We then use a prior spherical harmonic reconstruction as an initial solution.

The first stage of its reconstruction is the estimation of the axes of inertia of \mathcal{C}^* from the data, which provide the spherical harmonic modeling. The reconstructed harmonic surface is represented on Figure 3 (c) and corresponds to order $L = 3$ ($k = 16$ parameters). The computational complexity is related to the polyhedral approximation of the harmonic surface. Indeed, approximation of complex shapes requires a large number of vertices, and their projection evaluation become numerically expensive. Such argument clearly appears as a limitation of the harmonic method.

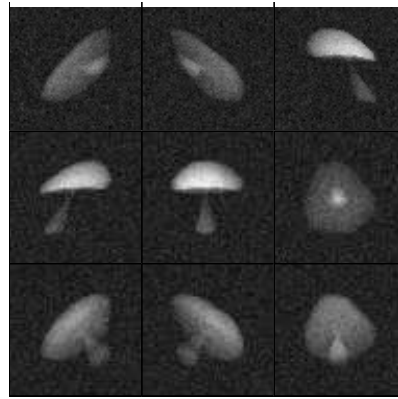
The polyhedron finally reconstructed with this harmonic surface as an initialization is plotted on Figure 3 (d). It is composed of $n = 95$ vertices and 186 triangular faces, and λ is selected empirically in order to avoid self intersected shapes while preserving the polyhedron smoothness. This reconstruction is very close to the real object, which is a significant proof of the ability of the first order spline model to reconstruct complex shapes.

6. CONCLUSIONS

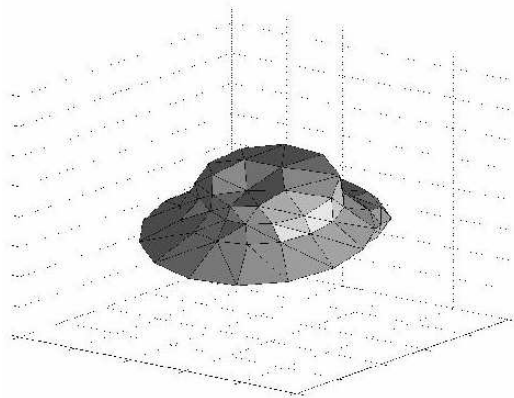
We have addressed the problem of closed surface reconstruction from X-ray tomographic data and we have studied the reconstruction of several parametric shapes. Global models, such as harmonic surfaces may not be efficient to retrieve complex shapes, whereas local ones, as splines, appear accurate to model shapes with inhomogeneous features. However, we have shown the interest of spherical harmonics since they yield star-shaped, and then



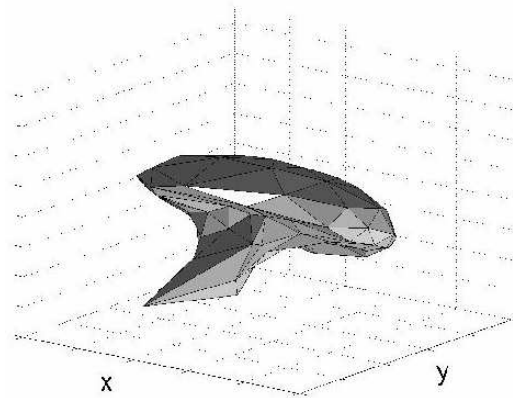
(a) Real object C^* and projection geometry



(b) Synthetic data



(c) Harmonic reconstruction



(d) Polyhedral reconstruction ($n = 95, \lambda = 2$)

Fig. 3. Simulation results. The harmonic model depends on 16 parameters, and polyhedron (d) is obtained with (c) as an initialization.

unintersected surfaces. We use harmonic surfaces to provide accurate initializations of the more sophisticated polyhedral model. The overall performance of the polyhedral approach has been presented in a difficult case where both number and angles of projections are limited. The reconstruction result is satisfactory, although strongly related to the initial solution.

7. REFERENCES

- [1] K. D. Sauer, J. J. Sachs, and C. Klifa, "Bayesian estimation of 3-D objects from few radiographs," *IEEE Trans. Nuclear Sciences*, vol. 41, no. 5, pp. 1780–1790, Oct. 1994.
- [2] P. Cinquin and B. Chalmond, "Hip prosthesis design," *Lecture Notes in Medical Informatics*, vol. 16, pp. 195–200, 1982.
- [3] D. J. Rossi and A. S. Willsky, "Reconstruction from projections based on detection and estimation of objects – Parts I and II: Performance analysis and robustness analysis," *IEEE Trans. Acoust. Speech, Signal Processing*, vol. ASSP-32, no. 4, pp. 886–906, Aug. 1984.
- [4] K. M. Hanson and G. S. Cunningham, "Exploring the reliability of Bayesian reconstructions," *Medical Imaging: Image Processing, Proc. SPIE*, vol. 2434, pp. 416–423, 1995.
- [5] A. Matheny and D. B. Goldgof, "The use of three and four-dimensional surface harmonics for rigid and nonrigid shape recovery and representation," *IEEE Trans. Pattern Anal. Mach. Intell.*, vol. 17, no. 10, pp. 967–981, Oct. 1995.
- [6] X. L. Battle, G. S. Cunningham, and K. M. Hanson, "Tomographic reconstruction using 3D deformable models," *Phys. Med. Biol.*, vol. 43, pp. 983–990, 1998.
- [7] P. Milanfar, W. C. Karl, and A. S. Willsky, "Reconstructing binary polygonal objects from projections: A statistical view," *Comput. Vision and Graphics and Image Processing*, vol. 56, no. 5, pp. 371–391, Sept. 1994.
- [8] A. Mohammad-Djafari, "Binary polygonal shape image reconstruction from a small number of projections," *Elektrik*, vol. 5, no. 1, pp. 127–138, 1997.
- [9] C. Soussen and A. Mohammad-Djafari, "Multiresolution approach to the estimation of the shape of a 3D compact object from its radiographic data," in *Proc. SPIE, Mathematical Modeling, Bayesian Estimation, and Inverse Problems*, F. Prêteux, A. Mohammad-Djafari, and E. R. Dougherty, Eds., Denver, CO, USA, July 1999, pp. 150–160.
- [10] C. Soussen, *Reconstruction 3D d'un objet compact en tomographie*, Phd thesis, Université de Paris-Sud, France, Dec. 2000.